



Published in final edited form as:

J Cell Sci. 2005 June 15; 118(Pt 12): 2557. doi:10.1242/jcs.02395.

Laminin-6 assembles into multimolecular fibrillar complexes with perlecan and participates in mechanical-signal transduction via a dystroglycan-dependent, integrin-independent mechanism

Jonathan C. R. Jones^{1,2,*}, Kimberly Lane^{1,2}, Susan B. Hopkinson^{1,2}, Emilia Lecuona¹, Robert C. Geiger¹, David A. Dean¹, Eduardo Correa-Meyer¹, Meredith Gonzales^{1,2}, Kevin Campbell³, Jacob I. Sznajder¹, and Scott Budinger¹

¹ Division of Pulmonary Medicine, Feinberg School of Medicine, Northwestern University, Morton 4-616, 303 East Chicago Avenue, Chicago, IL 60611, USA

² Department of Cell and Molecular Biology, Feinberg School of Medicine, Northwestern University, Morton 4-616, 303 East Chicago Avenue, Chicago, IL 60611, USA

³ Howard Hughes Medical Institute, Roy J. and Lucille A. Carver College of Medicine, Department of Physiology and Biophysics, University of Iowa, 400 Eckstein Medical Research Building, Iowa City, IA 52242, USA

Summary

Mechanical ventilation is a valuable treatment regimen for respiratory failure. However, mechanical ventilation (especially with high tidal volumes) is implicated in the initiation and/or exacerbation of lung injury. Hence, it is important to understand how the cells that line the inner surface of the lung [alveolar epithelial cells (AECs)] sense cyclic stretching. Here, we tested the hypothesis that matrix molecules, via their interaction with surface receptors, transduce mechanical signals in AECs. We first determined that rat AECs secrete an extracellular matrix (ECM) rich in anastomosing fibers composed of the $\alpha 3$ laminin subunit, complexed with $\beta 1$ and $\gamma 1$ laminin subunits (i.e. laminin-6), and perlecan by a combination of immunofluorescence microscopy and immunoblotting analyses. The fibrous network exhibits isotropic expansion when exposed to cyclic stretching (30 cycles per minute, 10% strain). Moreover, this same stretching regimen activates mitogen-activated-protein kinase (MAPK) in AECs. Stretch-induced MAPK activation is not inhibited in AECs treated with antagonists to $\alpha 3$ or $\beta 1$ integrin. However, MAPK activation is significantly reduced in cells treated with function-inhibiting antibodies against the $\alpha 3$ laminin subunit and dystroglycan, and when dystroglycan is knocked down in AECs using short hairpin RNA. In summary, our results support a novel mechanism by which laminin-6, via interaction with dystroglycan, transduces a mechanical signal initiated by stretching that subsequently activates the MAPK pathway in rat AECs. These results are the first to indicate a function for laminin-6. They also provide novel insight into the role of the pericellular environment in dictating the response of epithelial cells to mechanical stimulation and have broad implications for the pathophysiology of lung injury.

Keywords

Matrix adhesion; Matrix receptors; Stretching

*Author for correspondence (j-jones3@northwestern.edu).

Introduction

In intact tissue, many types of epithelial cells are routinely subject to mechanical forces (Ingber, 2003; Wang et al., 1993). For example, urothelial cells covering the inner surface of the bladder experience cycles of stretching and contraction as the bladder fills and then discharges its contents, whereas epithelial cells that line the gut are subjected to waves of peristalsis within the alimentary canal. Endothelial cells in intact blood vessels are subject to and respond precisely to changes in hemodynamic shear stress (Davies et al., 2003; Shyy and Chien, 2002). Epithelial cells that cover the alveolar surface of the lungs are no exception and undergo cyclic mechanical deformation forces during tidal breathing, particularly following lung injury (Brower et al., 2000; Corbridge et al., 1990; Correa-Meyer et al., 2002; Edwards, 2001; Liu et al., 1999; Steinberg et al., 2002; Webb and Tierney, 1974). Moreover, in alveolar epithelial cells (AECs), mechanical stimulation is known to initiate signals that result in increases in DNA synthesis and the expression of certain growth-factor receptors, surfactant proteins and extracellular-matrix proteins (Edwards, 2001; Liu et al., 1999). In addition, certain pathological conditions are initiated when AECs are subjected to excessive external forces. In particular, ventilation of patients with lung injury leads to increased cell-membrane permeability, pulmonary edema and inflammation, and contributes to mortality in patients with acute respiratory distress syndrome (ARDS) (Brower et al., 2000; Corbridge et al., 1990; Edwards, 2001; Liu et al., 1999; Webb and Tierney, 1974).

Although it has been established that cells sense external forces, in part, through mechanosensitive channels and growth-factor-receptor circuitry, there are considerable data that indicate that certain mechanical signals are transduced via matrix cell-surface receptors, including the integrins (Blount, 2003; Chen et al., 1999; Hamill and Martinac, 2001; Hynes, 1992; Hynes, 2002; Ingber, 2003; Tschumperlin et al., 2004; Wang et al., 1993). However, whether matrix receptors and their ligands, including the laminins and laminin-binding proteins, mediate such mechanical-signal transduction by converting mechanical signals into chemical signals in the cytoplasm of a cell is not clear (Edwards, 2001; Liu et al., 1999; Nilius and Droogmans, 2001).

The composition of the matrix to which AECs adhere in the intact lung has been studied by several groups. Specifically, several laminin subunits have been identified in the matrix-rich basement membrane of AECs in vivo (Coraux et al., 2002; Mizushima et al., 1998; Pierce et al., 1998; Virtanen et al., 1996). This basement membrane is covered by a sheet of cells composed mainly of type-I (AT1, alveolar type-I pneumocytes) cells (Crapo et al., 1982). The squamous AT1 cells line ~95% of the alveolar surface area and are susceptible to oxidant stress (Crapo et al., 1982). They share the basement membrane with type-II (AT2, pneumocyte type II) cells, which are cuboidal and cover less than 5% of the alveolar surface (Crapo et al., 1982). The type-II cells produce surfactant, proliferate and differentiate into type I cells (Crapo et al., 1982; Fehrenbach, 2001; Uhal, 1997). In the basement membrane of the lung, subunits of laminin show precise, developmentally regulated patterns of expression (Coraux et al., 2002; Mizushima et al., 1998; Pierce et al., 1998; Virtanen et al., 1996). For example, laminin α 1 expression is restricted to early human lung morphogenesis, whereas the laminin α 5 is continuous from early lung development to adult life (Pierce et al., 1998; Virtanen et al., 1996). Moreover, the α 3 laminin subunit is expressed in the basement membrane of the alveoli of adult rat lung, where it localizes with β 1, γ 1 and β 2 subunits. Indeed, some authors have speculated that alveolar cells might express at least five laminin isoforms (Pierce et al., 1998). In addition, several matrix-receptor complexes have been identified in the developing and adult lungs. In particular, the α 2, α 3 and α 6 integrin subunits are found in developing alveolar tissue and in adult alveoli, and might serve in AEC adherence to laminins in the basement membrane (Virtanen et al., 1996). The β 4 integrin appears to be restricted to the

bronchi, where it assembles into hemidesmosome structures that tether bronchial airway epithelial cells to laminin 5 in the basement membrane (Michelson et al., 2000).

In this study, we used primary rat AECs to assay the molecular underpinning of cellular response to physical force. In particular, we tested the hypothesis that matrix molecules secreted by lung epithelial cells are crucial molecular links in the process of 'converting' a mechanical stress in the form of stretching into a cytoplasmic signal. We present the first analyses of the function and organization of laminin 6 secreted by epithelial cells and we provide data that implicate dystroglycan as a component of a complex that transduces mechanical signals. Moreover, our results reveal that a novel matrix fibrillar complex transduces mechanical signals that regulate the activity of p42/p44 mitogen-activated-protein kinase (MAPK) in rat AECs. Our data and conclusions contrast with those of others, who have stated that mechanotransduction does not require 'force-dependent biochemical processes within the cell or cell membrane' (Tschumperlin et al., 2004).

Materials and Methods

Cell culture

AECs were isolated from pathogen-free male Sprague-Dawley rats (200–225 g) as previously described (Correa-Meyer et al., 2002; Ridge et al., 1997). Briefly, the lungs were perfused via the pulmonary artery, lavaged and digested with elastase (3 U ml^{-1} ; Worthington Biochemical, Freehold, NJ). AECs were purified by differential adherence to immunoglobulin G (IgG) pretreated dishes and cell viability was assessed by trypan-blue exclusion (>95%). Cells were resuspended in Dulbecco's modified Eagle's medium (DMEM; Cellgro, Mediatech Inc., Herndon, CA) containing 10% fetal bovine serum (FBS; Hyclone, Logan, UT) with 2 mM glutamine, 100 U ml^{-1} penicillin, $0.25 \mu\text{g ml}^{-1}$ amphotericin B and $100 \mu\text{g ml}^{-1}$ streptomycin. Cells were seeded in six-well, 35 mm, elastomer-bottomed Bioflex[®] plates (Flexcell International, Meckesport, PA) or peptide-coated glass coverslips at a density of 0.5×10^6 cells cm^{-2} . Cells were incubated in a humidified atmosphere of 5% CO_2 , 95% air at 37°C. The day of isolation and plating is designated culture day 0 (zero). 804G cells were cultured as detailed previously (Riddelle et al., 1991).

Antibodies and other reagents

Polyclonal rabbit antisera against p42/p44 MAPK and activated (phosphorylated) p42/p44 MAPK were purchased from Cell Signaling Technology (Beverly, MA). The mouse monoclonal antibodies CM6 and 5C5 against the laminin $\alpha 3$ subunit were described previously (Baker et al., 1996; Langhofer et al., 1993). Mouse monoclonal antibodies against the $\gamma 2$ and $\beta 3$ subunits of rat laminin 5 were originally provided by Desmos (San Diego, CA). A rabbit antiserum against the $\beta 1$ laminin subunit was obtained from P. Yurchenco (Department of Pathology, Robert Wood Johnson Medical School, Piscataway, NJ). Mouse monoclonal antibody (mAb) against the $\gamma 1$ laminin subunit (mAb 1920) was obtained from Chemicon International (Temecula, CA). A goat polyclonal antiserum against the $\alpha 5$ laminin subunit (G20) was purchased from Santa Cruz Biotechnology (Santa Cruz, CA). A rabbit antiserum against nidogen was obtained from Calbiochem (San Diego, CA). A hamster mAb (Ha2/5) that inhibits the function of rat $\beta 1$ integrin was purchased from BD Pharmingen (Franklin Lakes, NJ). A function-inhibitory rat antibody against $\alpha 3$ integrin (Ralph 3.1), a mouse mAb against the $\beta 2$ laminin subunit and mouse mAb against perlecan were obtained from the Developmental Studies Hybridoma Bank (University of Iowa, Iowa City, IA). Mouse IgM IIH6 against α -dystroglycan has been described elsewhere (Henry et al., 2001). Mouse mAb 8D5 against β -dystroglycan was purchased from Novocastra Labs (Newcastle, UK). Mouse IgM Ab1 against actin was purchased from Calbiochem. Control IgGs and IgMs, and fluorescein, rhodamine and horseradish-peroxidase-conjugated secondary antibodies were purchased from Jackson

ImmunoResearch (West Grove, PA). For imaging of unfixed matrix proteins under stretching, we labeled the matrix with the antibody 5C5 followed by Alexa-Fluor-488-conjugated goat anti-mouse IgG (Molecular Probes, Eugene, OR).

The GRGDSP peptide was purchased from Invitrogen (Carlsbad, CA) and added to the medium of the AECs at a concentration of $100 \mu\text{g ml}^{-1}$ in serum-free medium for 24 hours before stretching.

short hairpin RNA protocol

A set of single-stranded oligonucleotides encoding the dystroglycan target short hairpin RNA (shRNA) and its complement were synthesized by Invitrogen (Carlsbad, CA).

2719Forward: CACCGCTCATTGCTGGAATCATTGCCGAAGCAATGATTCCA-GCAATGAGC
2719Reverse:

AAAAGCTCATTGCTGGAATCATTGCTTCGGCAATGATTCCA-GCAATGAGC

The sequence was selected using an algorithm provided by Invitrogen. The oligonucleotide pair was annealed, ligated into the pENTR/U6 vector and used to transform competent *Escherichia coli* cells following an established protocol (Invitrogen). Plasmid DNA was isolated from the kanamycin-resistant colonies and sequenced. The pENTRY/U6 construct was used in a recombination reaction with the adenoviral vector pAD/BLOCK-iT-DEST (Invitrogen). The resulting shRNA adenoviral vector was linearized with *PacI* and transfected into 293A cells using Lipofectamine following Invitrogen protocols. In addition, an adenoviral vector containing shRNA targeting human (but not rat) lamin A/C (supplied by Invitrogen) was processed the same way and used as a negative control for the adenoviral infection. Approximately 12 days after transfection, the adenovirus-containing 293A cells were harvested and lysed to prepare a crude viral stock. The resultant viral stock was amplified and the viral concentration determined. 2 days after plating, AECs were infected with the virus at a multiplicity of infection of 1:10. The following day, the medium was replaced and assays were performed 24 hours later.

Cyclic stretching

AECs were cultured for 3 days. After serum starvation for 24 hours, the cells were subjected to equibiaxial stretching on day 4 using the Cyclic Strain Unit FX-3000 (Flexcell International, Hillsborough, NC). This unit consists of a controlled vacuum unit and a base plate to hold the culture plates. A vacuum was cyclically applied to elastomer-bottomed six-well culture dishes using the Flexercell device with loading stations in place to impose equibiaxial stretching at 30 cycles per minute and a stretching-relaxation ratio of 1:1, resulting in a 10% linear elongation of the membrane as measured microscopically. This is the same regimen used previously (Correa-Meyer et al., 2002). Cells were harvested at 10 minutes, after the initiation of cyclic stretching.

SDS-PAGE and immunoblotting

AECs were solubilized in sample buffer consisting of 8 M urea, 1% sodium dodecyl sulfate in 10 mM Tris-HCl, pH 6.8, 15% β -mercaptoethanol (Laemmli, 1970). AEC matrix was prepared according to a previously published procedure (Langhofer et al., 1993). The matrix proteins were collected from the culture dish by solubilization in the above sample buffer. Proteins were separated by SDS-PAGE, transferred to nitrocellulose and processed for immunoblotting as previously described (Harlow and Lane, 1988; Klatte et al., 1989; Laemmli, 1970). Immunoblots were scanned and quantified using Molecular Analyst (BioRad, Richmond, CA).

Immunofluorescence microscopy

Cells on glass coverslips were extracted for 2 minutes at -20°C in acetone. Cells maintained on elastomer surfaces in six-well plates were fixed in 3.7% formaldehyde for 5 minutes, extracted in 0.5% Triton X-100 in PBS at 4°C for 8 minutes in situ and then washed thoroughly in PBS. Subsequently, the elastomer surface with attached cells was excised from the six-well plate and processed as if it were a coverslip. Appropriate single primary antibodies or mixtures were overlaid onto the cells and the preparations were incubated at 37°C for 60 minutes. The cells on coverslips or elastomer were washed in three changes of PBS and then overlaid with secondary antibodies, placed at 37°C for an additional 60 minutes, washed extensively and then mounted on slides (cells on coverslips) or covered with a glass coverslip (cells on elastomer membrane). All preparations were viewed on a Zeiss laser-scanning confocal microscope (LSM 510) (Carl Zeiss, Thornwood, NY). Microscope images were exported as TIF files and figures were generated using Adobe Photoshop software.

Image analyses of $\alpha 3$ laminin under stretching

AECs were cultured on elastomer membranes (Flexcell International) for 4 days. AEC matrix was prepared according to a previously published procedure and then incubated at 37°C for 60 minutes in an unfixed state using mAb 5C5 against the $\alpha 3$ laminin subunit (Langhofer et al., 1993). After thorough washing in PBS, the membrane was incubated in Alexa-Fluor-488-conjugated goat anti-mouse IgG for an additional 60 minutes at 37°C . The membrane was mounted in a StageFlexer system (Flexcell International) on the stage of a Leica DMRXA2 microscope (Leica Microsystems, Wetzlar, Germany) coupled to a Hamamatsu Orca-ER digital camera (Hamamatsu, Bridgewater, NJ). This allowed the fibers to be viewed while they were undergoing cyclic stretching. The membranes were stretched as described above and images captured using OpenLab in both stretched and unstretched conformations. Measurements of fiber length and areas between fibers were generated by identifying fiducial points in the images, which were subsequently analyzed using the MetaMorph Imaging System (Universal Imaging, Molecular Devices, Downingtown, PA) by examining the same networks under stretching and non-stretching conditions. Significant differences between experimental conditions were analysed using a two-way analysis of variance (ANOVA). When the ANOVA indicated a significant difference between groups, individual differences were explored with two-tailed paired Student's *t*-tests using the Bonferroni correction for multiple comparisons. A significant difference was prospectively identified as $P < 0.05$.

Results

Primary AECs assemble a fibrous matrix enriched in perlecan, nidogen and laminin 6

To evaluate the potential role of extracellular matrix components in mechanotransduction in lung epithelial cells, we first characterized the composition of an extensive network of fibers that AECs deposit on their substrate (Figs 1, 2). At 2 days after plating, we detect small fibers, recognized by antibodies against perlecan along the substrate-attached surface of AECs (Fig. 1A). By contrast, antibodies against the $\beta 1$, $\gamma 1$ and $\alpha 3$ laminin subunits show either diffuse or punctate staining in the cells at the same focal plane at this time point (Fig. 1B; only perlecan and the $\beta 1$ -laminin-subunit staining is shown in this image). It should be realized that some of the $\beta 1$ -laminin-subunit-positive spots co-localize with the small fibers of perlecan (seen as yellow in Fig. 1C).

By day 4, perlecan appears in an extensive anastomosing network within the matrix of the cells (Fig. 1D). These perlecan-rich fibers are also stained by antibodies against the $\beta 1$, $\gamma 1$ and $\alpha 3$ laminin subunits and nidogen (Fig. 1E, Fig. 2A-F, Fig. 3). Other antibodies against laminin subunits, including those that recognize rat $\gamma 2$ and $\beta 3$ subunits, generate no obvious staining of cells at all time points we analysed, indicating that, in vitro, AECs fail to secrete a matrix

rich in laminin 5 ($\alpha 3\beta 3\gamma 2$) (data not shown). Antibodies against the $\alpha 5$ laminin subunit [a component of laminins 10 and 11 ($\alpha 5\beta 1\gamma 1$ and $\alpha 5\beta 2\gamma 1$)] and the $\beta 2$ -laminin subunit [a component of laminins 7 and 11 ($\alpha 3\beta 2\gamma 1$ and $\alpha 5\beta 2\gamma 1$)] stain AEC cell bodies and show only weak, diffuse staining of the AEC matrix (Fig. 2J, only $\beta 2$ laminin antibody staining is shown). Both $\alpha 5$ and $\beta 2$ laminin subunit antibodies fail to stain the perlecan/nidogen/ $\alpha 3$ -laminin-subunit-rich fibers secreted by the cells (Fig. 2J-L, only $\beta 2$ -laminin antibody staining is shown). These data suggest that the laminin-positive fibers in the matrix of AECs are rich in laminin 6 but lack laminins 7, 10 and 11.

In support of the immunofluorescence data, western blotting confirms that primary AECs express a distinct subset of laminin subunits. Antibodies against $\alpha 3$, $\beta 1$, $\beta 2$ and $\gamma 1$ laminin recognize proteins of 190 kDa and 160 kDa, 200 kDa, 190 kDa, and 200 kDa (respectively) in immunoblots of AEC extracts, whereas antibodies against other laminin subunits including $\gamma 2$ and $\beta 3$ show no obvious reactivity against the same protein preparation (Fig. 4). The latter antibodies, however, show strong reactivity with extracts derived from the rat bladder-cell line 804G, which is known to secrete a laminin-5-rich matrix (Baker et al., 1996; Langhofer et al., 1993) (Fig. 4A). It should be realized that we detect $\beta 2$ laminin subunit in extracts of 804G cells even though this protein is not deposited into the matrix that 804G cells secrete onto their culture support (J. C. R. Jones et al., unpublished).

We have previously demonstrated that post-translational proteolytic processing of the $\alpha 3$ laminin subunit can alter cellular responses to laminin-rich matrix (Goldfinger et al., 1998). In whole-cell extracts of AECs, both unprocessed (190 kDa) and processed (160 kDa) $\alpha 3$ laminin subunit isoforms are present (Amano et al., 2000; Goldfinger et al., 1999; Goldfinger et al., 1998; Nguyen et al., 2000) (Fig. 4A). In sharp contrast to this, only processed $\alpha 3$ laminin subunit is detectable in AEC matrix, indicating that $\alpha 3$ laminin has undergone extracellular proteolytic cleavage in its G domain upon secretion (Amano et al., 2000; Goldfinger et al., 1999; Goldfinger et al., 1998; Nguyen et al., 2000) (Fig. 4B).

Matrix and matrix-receptor involvement in the transduction of mechanical signals

A major goal of our study was to investigate whether mechanotransduction in AECs might involve matrix-receptor complexes (Chen et al., 1999; Ingber, 2003; Meyer et al., 2000; Pavalko et al., 1998; Shyy and Chien, 2002). Indeed, we hypothesized that the fibrous nature of the matrix of AECs might facilitate the transduction of stretching stimuli to adherent cells if it were to deform upon mechanical stimulation. To evaluate this possibility experimentally, we first subjected native AEC matrix to an equibiaxial stretch regimen (a linear 10% elongation at a frequency of 30 cycles per minute, with a stretching:relaxation ratio of 1:1), which Correa-Meyer et al. have previously shown elicits specific signaling events in AECs (Correa-Meyer et al., 2002). We chose to stimulate the matrix of AECs mechanically at 4 days after plating because, by this time, the AECs have established the same extensive fibrillar matrix on elastomer membranes that we observe when the cells are plated onto glass coverslips (compare Figs 1–3 with Fig. 5). $\alpha 3$ -Laminin subunits in unfixed, native AEC matrix were immunolabeled. The labeled preparation was visualized before stretching, during the stretching regimen mentioned previously and following stretching in liquid medium. An overlay of three images of the labeled matrix fibers under these distinct conditions is shown (Fig. 6A).

Before and after stretching, the $\alpha 3$ -laminin-subunit-rich fibers show colocalization, whereas the same fibers are displaced from their non-stretched organization upon mechanical stimulation (Fig. 6A). Upon exposure to cyclic stretching, the overall shape of the matrix network is not appreciably altered (Fig. 6A). Indeed, this suggests that the matrix fibers adhere to the substrate continuously or at multiple, closely spaced, points along their length. It should also be realized that stretching causes no obvious damage to or fragmentation of the matrix.

We next derived measurements of the changes in area enclosed by the fibers (A/A_0 ; where A is the area during stretching and A_0 is the area before stretching) and the length of the fibers (L/L_0 ; where L is the fiber length during stretching and L_0 is the fiber length before stretching) in the matrix of AECs (Fig. 6B). Both fiber area and fiber length are increased significantly during stretching, and return more or less to the baseline after cessation of stretching.

A tightly adherent matrix undergoing equibiaxial stretch should exhibit isotropic expansion. To determine whether AEC matrix does so, we used the formula

$$\Lambda = (A/A_0) \div (L/L_0)^2,$$

where Λ is a numerical value for expansion. Values for each of our measurements were calculated and then the average was generated. The resulting ratio is 1.03 (95% confidence interval 0.76–1.30). Statistically, the ratio is essentially 1, the predicted value for an ideal, isotropic expansion.

When AECs are subjected to the stretching regimen mentioned above, p42/p44 MAPK undergoes activation within 15 minutes (Correa-Meyer et al., 2002). Hence, we were able to use this endpoint, in combination with a collection of function-blocking antibodies to define which particular matrix components play a role in stretching-induced signaling in AECs. AECs were washed with serum-free medium and then incubated in the same medium with antibody or control immunoglobulin for 24 hours before applying the regimen of cyclic stretching. Extracts of cells were processed for immunoblotting using antibodies that recognize activated p42/p44 MAPK, and then reprobbed with antibodies against total p42/p44 MAPK. We show pairs of images of one representative immunoblot and quantification of at least three trials of each experimental treatment (Fig. 7).

Inhibiting the function of the $\alpha 3$ laminin subunit results in a ~40% decrease in stretching-induced p42/p44 MAPK phosphorylation (Baker et al., 1996) (Fig. 7A, B). By contrast, blocking the function of either $\alpha 3$ or $\beta 1$ integrin with antibody antagonists has no obvious impact on stretching-activated p42/p44 MAPK phosphorylation (Fig. 7A, B). These same inhibitors are functionally active against rat integrins in our hands, because both inhibit rat 804G bladder-cell adhesion to laminin 5 in a 30 minute adhesion assay (J. C. R. Jones, unpublished).

Our data showing expression of dystroglycan by AECs suggest that dystroglycan might function as a receptor for the perlecan/laminin-6 complexes (Fig. 4C). This hypothesis is supported by the observation that the α -dystroglycan function-perturbing antibody IIIH6 effectively inhibits stretching-induced MAPK activation in AECs by about 30% (Michele and Campbell, 2003) (Fig. 7A, B). To confirm this result, we infected AECs 2 days after plating with adenovirus encoding shRNA to knockdown specifically the production of dystroglycan (Fig. 7C) (Elbashir et al., 2002). Knockdown of dystroglycan is >90% in AECs 2 days after infection (Fig. 7C). At the same time, we then assayed dystroglycan-shRNA and control-shRNA-expressing cells for MAPK activity following stretch (Fig. 7B). MAPK activation is inhibited by at least 50% in AECs in which production of dystroglycan is knocked down compared with untreated cells and cells expressing control shRNA (Fig. 7B).

It should be realized that AECs show no obvious morphological perturbation, including detachment or rounding, following treatment with any of the function-perturbing antibodies we used in these studies, or following treatment with adenovirus (not shown). Furthermore, laminin-6-fiber organization is not perturbed by our antibody or viral regimens. Moreover, the same approximate amount of total cell protein is collected from cultures of untreated cells and

cells treated with antibodies or adenovirus at the conclusion of the stretch regimen (not shown). Together, these results indicate that no obvious loss or death of cells is caused by antibody incubation or viral infection.

Irrelevant IgG and IgM treatment has no impact on activation of MAPK in AECs subject to stretching (not shown). We have performed several other control studies to assess the specificity of matrix molecule involvement in transducing mechanical signals in the AECs. For example, AECs 3 days after plating were incubated with an excess of RGD-containing peptide in serum-free medium and then, 24 hours later, the treated cells were subjected to stretch (Fig. 7B). This peptide is a competitive inhibitor of the receptor-binding site on matrix molecules including fibronectin and vitronectin for several $\beta 1$ - and $\beta 3$ -subunit-containing integrin-family members (Hynes, 1992). The RGD-containing peptide does not inhibit stretching-induced p42/p44 MAPK activation in AECs, indicating that RGD-binding integrins, including $\alpha 5\beta 1$ and $\alpha v\beta 3$, are not involved in mediating signaling in the stretched cells. Rather, our results suggest roles for laminin-6, the proteoglycan perlecan and dystroglycan in mediating stretching-induced signaling in AECs.

Discussion

The alveolar cells of the lung lie on a basement membrane composed of a complex of matrix proteins (Miner et al., 1997; Nguyen et al., 2002). In the intact lung, the production of laminin subunits is developmentally regulated. For example, the $\alpha 1$ and $\alpha 2$ subunits are expressed in fetal lungs, whereas $\alpha 3$, $\alpha 4$ and $\alpha 5$ laminin subunits are found in both fetal and adult lungs. Previous workers have shown that both $\alpha 3$ and $\alpha 5$ laminin subunits are produced by cultured rat AECs (Pierce et al., 1998). However, the exact identity of the $\alpha 3$ -subunit-containing laminin heterotrimer in the matrix of AECs has not been reported. Here, we provide the first evidence that the $\alpha 3$ laminin subunit is secreted by cultured rat AECs in cable-like structures. Moreover, we detect the $\beta 1$ and $\gamma 1$, but not the $\gamma 2$, $\beta 2$ and $\beta 3$ laminin subunits, localized with the $\alpha 3$ laminin subunit in these cables, indicating that the rat cells are generating a laminin-6-rich matrix. To our knowledge, this is the first identification of a cell type that secretes a laminin-6-rich matrix in the absence of laminin 5 or 7 in vitro. Moreover, we have been able to use AECs to study not only the precise organizational state of laminin 6 in the extracellular matrix but also the role of laminin 6 as a mediator of signaling.

Laminin heterotrimers assemble into polymeric matrix arrays in distinct ways in different cultured cell types. For example, in the rat epithelial cell line 804G, laminin 5 assembles into a “cat’s-paw” array, whereas the same molecule assembles in cloud-like arrays, arcs and circles in the matrix of keratinocytes (deHart et al., 2003; Langhofer et al., 1993). By contrast, laminin 1 assembles as a reticular network on the surface of muscle cells (Colognato et al., 1999), and the organizational state of laminin 6 in AEC matrix resembles this. Exactly how laminin 6 assembles into cable-like structural arrays remains to be determined. However, our time-course studies suggest that perlecan is laid down in a fibrillar organization before laminin 6. Indeed, we speculate that AECs first assemble fibers of perlecan whose distribution subsequently determines the arrangement of laminin 6. Perlecan is certainly capable of doing so via an interaction with nidogen, which cross-links the immunoglobulin-like domain 3 of perlecan with an epidermal-growth-factor-like repeat within the laminin $\gamma 1$ subunit (Kvansakul et al., 2001; Mayer et al., 1993; Ries et al., 2001). In support of this, we show that nidogen codistributes with perlecan and the subunits of laminin 6 in the matrix of AECs.

The fibrous nature of perlecan/nidogen/laminin-6-rich complexes in the matrix of AECs led us to ask whether these fibers provide the structural means for cells to resist and/or respond to mechanical stresses. Indeed, by visualizing labeled fibers, we have shown that the fibers adhere to the matrix at sites sufficiently close to one another to result in isotropic expansion during

stretching. Hence, the ability of fibers rich in laminin 6 to respond to stretching by undergoing a precise deformation makes them ideal transducers of force from the outside to the inside of cells, initiating signaling cascades that, in turn, trigger specific physiological responses (Gillespie and Walker, 2001). To test this hypothesis, we used activation of the p42/p44 MAPK pathway as our endpoint. This important cytoprotective signal pathway is maximally activated within 15 minutes of the initiation of cyclic stretching in AECs (Correa-Meyer et al., 2002). Using an antibody that we have previously shown to bind to and inhibit the function of the $\alpha 3$ laminin subunit, we have provided evidence that laminin 6 is one link in the molecular pathway that transmits an outside-in mechanical signal (Baker et al., 1996). It should be realized that this pathway is distinct from the recently detailed growth-factor-receptor circuitry involved in mechanical signaling in bronchial airway cells (Tschumperlin et al., 2004).

We initially assumed that laminin 6 would transduce a signal via its interaction with an integrin at the surface of AECs, because the role of integrins in signal transduction is well established (Howe et al., 1998; Hynes, 1992; Hynes, 2002). There are several potential integrin receptors for laminins containing the $\alpha 3$ laminin subunit, including the integrin heterodimers $\alpha 6\beta 4$, $\alpha 3\beta 1$ and $\alpha 6\beta 1$ (Carter et al., 1991; Jones et al., 1998). Our primary AECs do not produce the $\beta 4$ integrin subunit, as assessed by immunoblotting and immunofluorescence using a polyclonal antibody against the $\beta 4$ integrin subunit that recognizes $\beta 4$ integrin in rat bladder cells (not shown). By contrast, rat AECs produce $\beta 1$ -containing integrin heterodimers. Thus, we focused on testing the hypothesis that $\beta 1$ -subunit-containing integrin heterodimers mediate the signal initiated by stretching that impacts MAPK activation in AECs. We did so using an antibody that inhibits rat $\beta 1$ -integrin function. However, function-perturbing antibodies against both $\beta 1$ and $\alpha 3$ integrins, as well as the RGD peptide, which inhibit the activity of a range of integrin receptors, fail to block stretching-induced p42/p44 MAPK activation in AECs (Hynes, 1992; Hynes, 2002).

If integrins are not involved in mediating mechanical signaling in AECs, what senses matrix deflections at the surface of these cells? A candidate receptor for mediating laminin-6 signaling is dystroglycan. Dystroglycan is best known as a component of the dystrophin-glycoprotein complex, whose absence or abnormality leads to muscular dystrophies and several types of cardiomyopathy (Michele and Campbell, 2003). This complex plays a structural role in muscle by forming a mechanically strong link between the sarcolemma and actin, but whether it transduces signals is controversial (Michele and Campbell, 2003; Rybakova et al., 2000; Spence et al., 2004). When bound to laminin, dystroglycan is reported to inhibit MAPK activation (Ferletta et al., 2003). In epithelial cells, the functions of dystroglycan are not clear, although it is believed to be primarily a structural protein involved in basement-membrane assembly, growth control, cytoskeleton organization, development of cell polarity and epithelial morphogenesis (Durbeej et al., 2001; Muschler et al., 2002).

Our study provides the first evidence that dystroglycan is a component of a distinct molecular pathway that transduces mechanical signals from the outside to the inside of AECs. The binding site for dystroglycan on laminins resides within the C-terminal G-domain modules of the α laminin subunit (Ido et al., 2004). Hence, because the $\alpha 3$ subunit lacks these modules, we presume that dystroglycan does not directly bind laminin 6 in the matrix of AECs (Ferletta et al., 2003; Timpl et al., 2000; Yu and Talts, 2003). Rather, dystroglycan probably interacts with the perlecan secreted by AECs. Indeed, previous biochemical data and the results of the present study support a model for integrin-independent, matrix-driven mechanotransduction in AECs. In our model, perlecan binds dystroglycan located in the membrane of AECs and interacts with laminin 6 in the matrix via nidogen (Talts et al., 1999) (Fig. 8). Moreover, our data indicate that stretching induces deformational changes in the supramolecular organization of the copolymers of laminin 6 and perlecan. Furthermore, we hypothesize that the proteoglycan perlecan relays these changes at the surface of AECs via its interaction with dystroglycan. At

the surface of AECs, dystroglycan is the direct mediator of mechanical signaling and activates p42/p44 MAPK (Fig. 8). The ability of dystroglycan to regulate MAPK might relate to their existence as a complex at the cell surface, evidence for which has recently been reported (Spence et al., 2004).

In summary, analyses of AECs and their response to stretching support a major role for dystroglycan in mediating integrin-independent, matrix-driven mechanotransduction in AECs. Our studies hold implications not only for the ways epithelial cells sense and respond to mechanical stimulation in general but also for the pathophysiology of certain lung diseases. Specifically, AECs undergo stretching when the lung is mechanically ventilated with high lung volumes. This might be injurious, leading to the failure of the epithelial sheet that covers the lung surface (Liu et al., 1999). Our results suggest that mechanically induced MAPK activation functions as a protective mechanism to ameliorate potential damage caused by overdistention of AECs. There is precedent for this because activation of MAPK pathways is known to promote the survival of several cell types, most notably in the nervous and immune systems (Bonni et al., 1999; Holmström et al., 2000). Defining the precise molecular pathway(s) by which AECs respond to mechanical stretching and elicit survival signals might lead to the design of strategies to protect the alveolar epithelium against injury induced by positive-pressure ventilation (Matthay et al., 2003; Sznajder, 2001).

Acknowledgments

This work was supported by grants RO1 DK60589 (J.C.R.J.) and PO1 HL 071643 (J.C.R.J., S.B., D.A.D. and J.I.S.) from the NIH. We are grateful to the Core of the latter grant for providing cells for our studies. We thank M. Glucksberg and T.-L. Chew for their great help in data analyses. We are most grateful to P. Yurchenco for his generous gift of antibodies.

References

- Amano S, Scott IA, Takahara K, Koch M, Gerecke DR, Keene DR, Hudson DL, Nishiyama T, Lee S, Greenspan DS, et al. Bone morphogenetic protein-1 (BMP-1) is an extracellular processing enzyme of the laminin 5 γ 2 chain. *J Biol Chem* 2000;275:22728–22735. [PubMed: 10806203]
- Baker SE, Hopkinson SB, Fitchmun M, Andreason GL, Frasier F, Plopper G, Quaranta V, Jones JCR. Laminin-5 and hemidesmosomes: role of the alpha 3 chain subunit in hemidesmosome stability and assembly. *J Cell Sci* 1996;109:2509–2520. [PubMed: 8923212]
- Blount P. Molecular mechanisms of mechanosensation: big lessons from small cells. *Neuron* 2003;37:731–734. [PubMed: 12628164]
- Bonni A, Brunet A, West AE, Datta SR, Takasu MA, Greenberg ME. Cell survival promoted by the Ras-MAPK signaling pathway by transcription-dependent and -independent mechanisms. *Science* 1999;286:1358–1362. [PubMed: 10558990]
- Brower RG, Matthay MA, Morris A, Schoenfeld D, Taylor Thompson B, Wheeler A. Ventilation with lower tidal volumes as compared with traditional tidal volumes for acute lung injury and the acute respiratory distress syndrome. The Acute Respiratory Distress Syndrome Network. *New Engl J Med* 2000;342:1301–1308. [PubMed: 10793162]
- Carter WG, Ryan MC, Gahr PJ. Epiligrin, a new cell adhesion ligand for integrin α 3 β 1 in epithelial basement membranes. *Cell* 1991;65:599–610. [PubMed: 2032285]
- Chen KD, Li YS, Kim M, Li S, Yuan S, Chien S, Shyy JY. Mechanotransduction in response to shear stress. Roles of receptor tyrosine kinases, integrins, and Shc. *J Biol Chem* 1999;274:18393–18400. [PubMed: 10373445]
- Colognato H, Winkelmann DA, Yurchenco PD. Laminin polymerization induces a receptor-cytoskeleton network. *J Cell Biol* 1999;145:619–631. [PubMed: 10225961]
- Coraux C, Meneguzzi G, Rousselle P, Puchelle E, Gaillard D. Distribution of laminin 5, integrin receptors, and branching morphogenesis during human fetal lung development. *Dev Dyn* 2002;225:176–185. [PubMed: 12242717]

- Corbridge TC, Wood LD, Crawford GP, Chudoba MJ, Yanos J, Sznajder JI. Adverse effects of large tidal volume and low PEEP in canine acid aspiration. *Am Rev Respir Dis* 1990;142:311–315. [PubMed: 2200314]
- Correa-Meyer E, Pesce L, Guerrero C, Sznajder JI. Cyclic stretch activates ERK1/2 via G-proteins and epidermal growth factor receptor in alveolar epithelial cells. *Am J Physiol* 2002;282:L883–L891.
- Crapo JD, Barry BE, Gehr P, Bachofen M, Weibel ER. Cell number and cell characteristics of the normal human lung. *Am Rev Respir Dis* 1982;26:332–337. [PubMed: 7103258]
- Davies PF, Zilberberg J, Helmke BP. Spatial microstimuli in endothelial mechanosignaling. *Circ Res* 2003;92:359–370. [PubMed: 12623874]
- deHart GW, Healy KE, Jones JCR. The role of $\alpha\beta 1$ integrin in determining the supramolecular organization of laminin-5 in the extracellular matrix of keratinocytes. *Exp Cell Res* 2003;283:67–79. [PubMed: 12565820]
- Durbeej M, Talts JF, Henry MD, Yurchenco PD, Campbell KP, Ekblom P. Dystroglycan binding to laminin alpha1LG4 module influences epithelial morphogenesis of salivary gland and lung in vitro. *Differentiation* 2001;69:121–134. [PubMed: 11798066]
- Edwards YS. Stretch stimulation: its effects on alveolar type II cell function in the lung. *Comp Biochem Physiol A* 2001;129:245–260.
- Elbashir SM, Harborth J, Weber K, Tuschl T. Analysis of gene function in somatic mammalian cells using small interfering RNAs. *Methods* 2002;26:199–213. [PubMed: 12054897]
- Fehrenbach H. Alveolar epithelial type II cell: defender of the alveolus revisited. *Resp Res* 2001;2:33–46.
- Ferletta M, Kikkawa Y, Yu H, Talts JF, Durbeej M, Sonnenberg A, Timpl R, Campbell KP, Ekblom P, Genersch E. Opposing roles of integrin alpha6Abeta1 and dystroglycan in laminin-mediated extracellular signal-regulated kinase activation. *Mol Biol Cell* 2003;14:2088–2103. [PubMed: 12802077]
- Gillespie PG, Walker RG. Molecular basis of mechanosensory transduction. *Nature* 2001;413:194–202. [PubMed: 11557988]
- Goldfinger LE, Stack MS, Jones JCR. Processing of laminin-5 and its functional consequences: role of plasmin and tissue-type plasminogen activator. *J Cell Biol* 1998;141:255–265. [PubMed: 9531563]
- Goldfinger LE, Hopkinson SB, deHart GW, Collawn S, Couchman JR, Jones JCR. The $\alpha 3$ laminin subunit, $\alpha 6\beta 4$ and $\alpha 3\beta 1$ integrin coordinately regulate wound healing in cultured epithelial cells and in the skin. *J Cell Sci* 1999;112:2615–2629. [PubMed: 10413670]
- Hamill OP, Martinac B. Molecular basis of mechanotransduction in living cells. *Physiol Rev* 2001;81:685–740. [PubMed: 11274342]
- Harlow, E.; Lane, D. *Antibodies: A Laboratory Manual*. Cold Spring Harbor; New York: 1988. Immunoblotting: p. 471-510.
- Henry MD, Satz JS, Brakebusch C, Costell M, Gustafsson E, Fassler R, Campbell KP. Distinct roles for dystroglycan, $\beta 1$ integrin and perlecan in cell surface laminin organization. *J Cell Sci* 2001;114:1137–1144. [PubMed: 11228157]
- Holmström TH, Schmitz I, Söderström TS, Poukkula M, Johnson VL, Chow SC, Krammer PH, Eriksson JE. MAPK/ERK signaling in activated T cells inhibits CD95/Fas-mediated apoptosis downstream of DISC assembly. *EMBO J* 2000;19:5418–5428. [PubMed: 11032809]
- Howe A, Aplin AE, Alahari SK, Juliano RL. Integrin signaling and cell growth control. *Curr Opin Cell Biol* 1998;10:220–231. [PubMed: 9561846]
- Hynes RO. Integrins: versatility, modulation, and signaling in cell adhesion. *Cell* 1992;69:11–25. [PubMed: 1555235]
- Hynes RO. Integrins: bidirectional, allosteric signaling machines. *Cell* 2002;110:673–687. [PubMed: 12297042]
- Ido H, Harada K, Futaki S, Hayashi Y, Nishiuchi R, Natsuka Y, Li S, Wada Y, Combs AC, Ervasti JM, et al. Molecular dissection of the alpha-dystroglycan and integrin-binding sites within the globular domain of human laminin-10. *J Biol Chem* 2004;279:10946–10954. [PubMed: 14701821]
- Ingber DE. Tensegrity II. How structural networks influence cellular information processing networks. *J Cell Sci* 2003;116:1397–1408. [PubMed: 12640025]

- Jones JCR, Hopkinson SB, Goldfinger LE. Structure and assembly of hemidesmosomes. *BioEssays* 1998;20:488–494. [PubMed: 9699461]
- Klatte DH, Kurpakus MA, Grelling KA, Jones JCR. Immunochemical characterization of three components of the hemidesmosome and their expression in cultured epithelial cells. *J Cell Biol* 1989;109:3377–3390. [PubMed: 2689457]
- Kvansakul M, Hopf M, Ries A, Timpl R, Hohenester E. Structural basis for the high-affinity interaction of nidogen-1 with immunoglobulin-like domain 3 of perlecan. *EMBO J* 2001;20:5342–5346. [PubMed: 11574465]
- Laemmli UK. Cleavage of structural proteins during assembly of the head of bacteriophage T4. *Nature* 1970;227:680–685. [PubMed: 5432063]
- Langhofer M, Hopkinson SB, Jones JCR. The matrix secreted by 804G cells contains laminin-related components that participate in hemidesmosome assembly in vitro. *J Cell Sci* 1993;105:753–764. [PubMed: 8408302]
- Liu M, Tanswell AK, Post M. Mechanical force-induced signal transduction in lung cells. *Am J Physiol* 1999;277:L667–L683. [PubMed: 10516207]
- Matthay MA, Zimmerman GA, Esmon C, Bhattacharya J, Collier B, Doerschuk CM, Floros J, Gimbrone MAJ, Hoffman E, Hubmayr RD, et al. Future research directions in acute lung injury: summary of a National Heart, Lung, and Blood Institute working group. *Am J Resp Crit Care Med* 2003;167:1027–1035. [PubMed: 12663342]
- Mayer U, Nischt R, Pöschl E, Mann K, Fukuda K, Gerl M, Yamada Y, Timpl R. A single EGF-like motif of laminins is responsible for high affinity nidogen binding. *EMBO J* 1993;12:1879–1885. [PubMed: 8491180]
- Meyer CJ, Alenghat FJ, Rim P, Fong JHJ, Fabry B, Ingber DE. Mechanical control of cyclic AMP signaling and gene transcription through integrins. *Nat Cell Biol* 2000;2:666–668. [PubMed: 10980709]
- Michele DE, Campbell KP. Dystrophin-glycoprotein complex: post-translational processing and dystroglycan function. *J Biol Chem* 2003;278:15457–15460. [PubMed: 12556455]
- Michelson P, Tigue M, Jones JCR. Human bronchial epithelial cells secrete laminin 5, express hemidesmosomal proteins and assemble hemidesmosomes. *J Histo Cytochem* 2000;48:535–544.
- Miner JH, Patton BL, Lentz SI, Gilbert DJ, Snider WD, Jenkins NA, Copeland NG, Sanes JR. The laminin alpha chains: expression, developmental transitions, and chromosomal locations of alpha1-5, identification of heterotrimeric laminins 8–11, and cloning of a novel alpha3 isoform. *J Cell Biol* 1997;137:685–701. [PubMed: 9151674]
- Mizushima H, Koshikawa N, Moriyama K, Takamura H, Nagashima Y, Hirahara F, Miyazaki K. Wide distribution of laminin-5 gamma 2 chain in basement membranes of various human tissues. *Horm Res* 1998;50 (Suppl 2):7–14. [PubMed: 9721586]
- Muschler J, Levy D, Boudreau R, Henry M, Campbell K, Bissell MJ. A role for dystroglycan in epithelial polarization: loss of function in breast tumor cells. *Cancer Res* 2002;62:7102–7109. [PubMed: 12460932]
- Nguyen BP, Gil SG, Carter WG. Deposition of laminin 5 by keratinocytes regulates integrin adhesion and signaling. *J Biol Chem* 2000;275:31896–31907. [PubMed: 10926936]
- Nguyen NM, Bai Y, Mochitate K, Senior RM. Laminin alpha-chain expression and basement membrane formation by MLE-15 respiratory epithelial cells. *Am J Physiol* 2002;282:L1004–L1011.
- Nilius B, Droogmans G. Ion channels and their functional role in vascular endothelium. *Physiol Rev* 2001;81:1415–1459. [PubMed: 11581493]
- Pavalko FM, Chen NX, Turner CH, Burr DB, Atkinson S, Hsieh YF, Qiu J, Duncan RL. Fluid shear-induced mechanical signaling in MC3T3-E1 osteoblasts requires cytoskeleton-integrin interactions. *Am J Physiol* 1998;275:C1591–C1601. [PubMed: 9843721]
- Pierce RA, Griffin GL, Mudd MS, Moxley MA, Longmore WJ, Sanes JR, Miner JH, Senior RM. Expression of laminin α 3, α 4 and α 5 chains by alveolar epithelial cells and fibroblasts. *Am J Respir Cell Mol Biol* 1998;19:237–244. [PubMed: 9698595]
- Riddelle KS, Green KJ, Jones JCR. Formation of hemidesmosomes in vitro by a transformed rat bladder cell line. *J Cell Biol* 1991;112:159–168. [PubMed: 1986003]

- Ridge K, Rutschman DH, Bertorello AM, Sznajder JI. Differential expression of Na-K-ATPase isoforms in rat alveolar epithelial cells. *Am J Physiol* 1997;273:L246–L255. [PubMed: 9252562]
- Ries A, Göhring W, Fox JW, Timpl R, Sasaki T. Recombinant domains of mouse nidogen-1 and their binding to basement membrane proteins and monoclonal antibodies. *Eur J Biochem* 2001;268:5119–5128. [PubMed: 11589703]
- Rybakova IN, Patel JR, Ervasti JM. The dystrophin complex forms a mechanically strong link between the sarcolemma and costameric actin. *J Cell Biol* 2000;150:1209–1214. [PubMed: 10974007]
- Shyy JYJ, Chien S. Role of integrins in endothelial mechanosensing of shear stress. *Circ Res* 2002;91:769–775. [PubMed: 12411390]
- Spence HJ, Dhillon AS, James M, Winder SJ. Dystroglycan, a scaffold for the ERK-MAP kinase cascade. *EMBO Rep* 2004;5:1–6. [PubMed: 14710173]
- Steinberg J, Schiller HJ, Halter JM, Gatto LA, Dasilva M, Amato M, McCann UG, Nieman GF. Tidal volume increases do not affect alveolar mechanics in normal lung but cause alveolar overdistension and exacerbate alveolar instability after surfactant deactivation. *Crit Care Med* 2002;30:2675–2683. [PubMed: 12483058]
- Sznajder JI. Alveolar edema must be cleared for the acute respiratory distress syndrome patient to survive. *Am J Resp Crit Care Med* 2001;163:1293–1294. [PubMed: 11371384]
- Talts JF, Andac Z, Gohring W, Brancaccio A, Timpl R. Binding of the G domains of laminin alpha1 and alpha2 chains and perlecan to heparin, sulfatides, alpha-dystroglycan and several extracellular matrix proteins. *EMBO J* 1999;18:863–870. [PubMed: 10022829]
- Timpl R, Tisi D, Talts JF, Andac Z, Sasaki T, Hohenester E. Structure and function of laminin LG modules. *Matrix Biol* 2000;19:309–317. [PubMed: 10963991]
- Tschumperlin DJ, Dai G, Maly IV, Kikuchi T, Laiho LH, McVittie AK, Haley KJ, Lilly CM, So PTC, Lauffenburger DA, et al. Mechanotransduction through growth-factor shedding into the extracellular space. *Nature* 2004;429:83–86. [PubMed: 15103386]
- Uhal BD. Cell cycle kinetics in the alveolar epithelium. *Am J Physiol* 1997;272:L1031–L1045. [PubMed: 9227501]
- Virtanen I, Laitinen A, Tani T, Paakko P, Laitinen LA, Burgeson RE, Lehto VP. Differential expression of laminins and their integrin receptors in developing and adult human lung. *Am J Respir Cell Mol Biol* 1996;15:184–196. [PubMed: 8703474]
- Wang N, Butler JP, Ingber DE. Mechanotransduction across the cell surface and through the cytoskeleton. *Science* 1993;260:1124–1127. [PubMed: 7684161]
- Webb HH, Tierney DF. Experimental pulmonary edema due to intermittent positive pressure ventilation with high inflation pressures. Protection by positive end-expiratory pressure. *Am Rev Respir Dis* 1974;110:556–565. [PubMed: 4611290]
- Yu H, Talts JF. Beta1 integrin and alpha-dystroglycan binding sites are localized to different laminin-G-domain-like (LG) modules within the laminin alpha5 chain G domain. *Biochem J* 2003;371:289–299. [PubMed: 12519075]

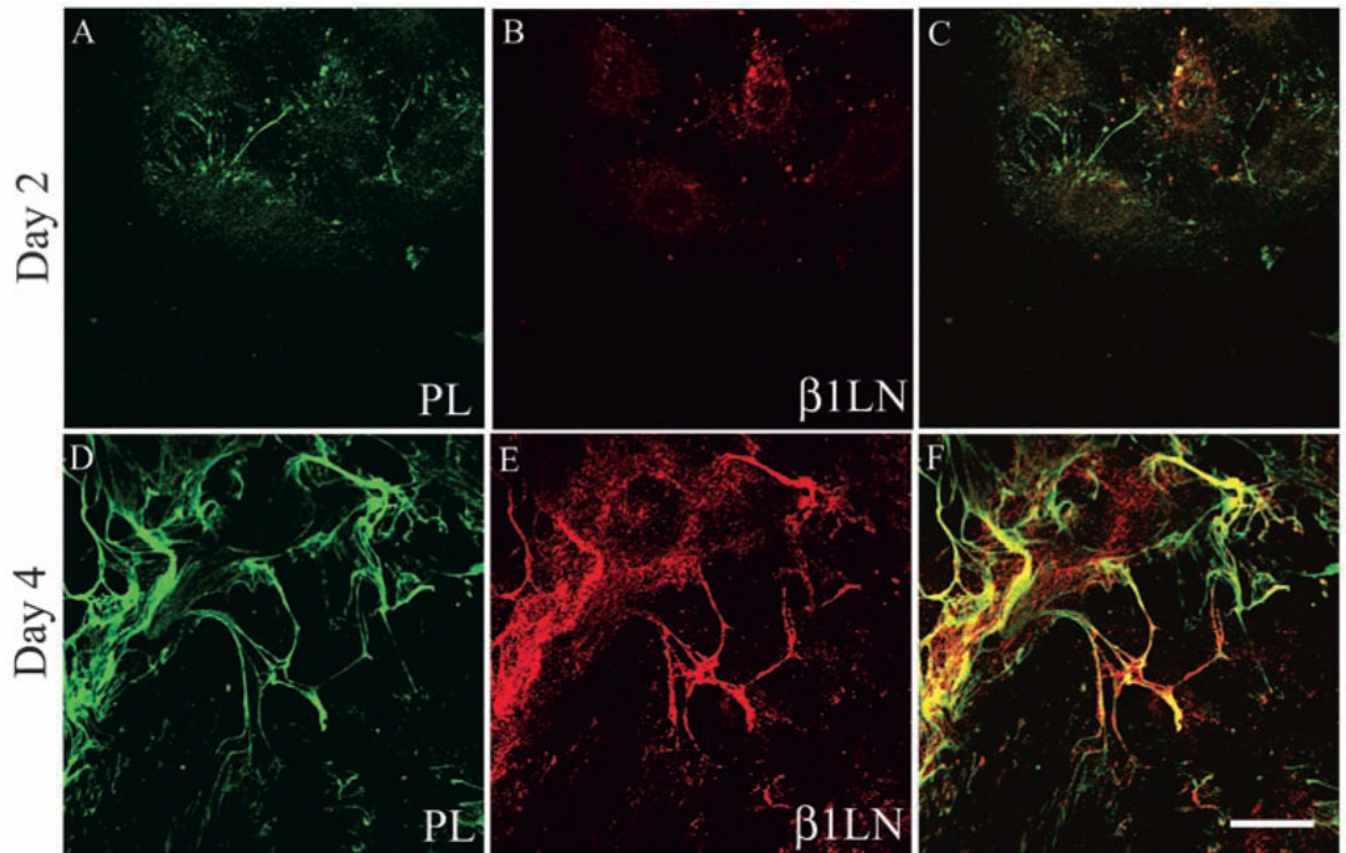


Fig. 1. Matrix organization of AECs. AECs at 2 and 4 days after isolation were processed for double-label indirect immunofluorescence microscopy using antibodies against perlecan (A, D) in combination with an antiserum against the $\beta 1$ laminin subunit (B, E). Images of cells were generated using confocal laser scanning microscopy. The focal plane was as close as possible to the substratum-attached surface of the cells. Areas of co-localization are indicated by the yellow color in the overlay images shown in C, F. Bar, 10 μm .

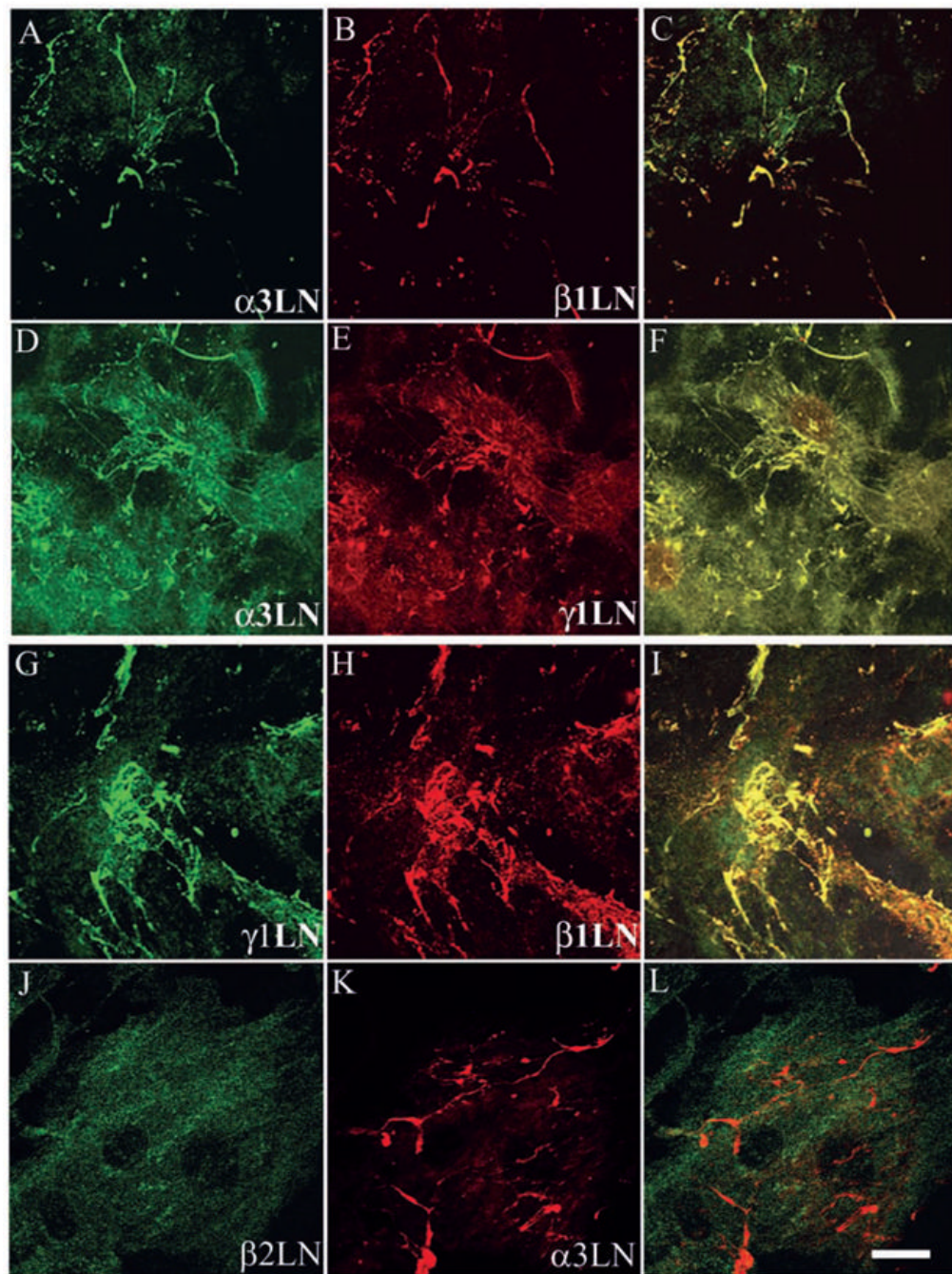


Fig. 2.

AECs maintained in culture secrete a laminin-6-rich matrix. AECs at 4 days after isolation were processed for double-label indirect immunofluorescence using antibodies against the $\alpha 3$ laminin subunit (A, D) in combination with antibodies against either $\beta 1$ laminin (B) or $\gamma 1$ laminin (E). (G-I) Cells were processed with a mix of antibodies against $\gamma 1$ and $\beta 1$ laminin subunits, as indicated. (J-L) Cells were processed with a mix of antibodies against $\alpha 3$ and $\beta 2$ laminin subunit, as indicated. Specimens were viewed by confocal laser-scanning microscopy with the focal plane being as close as possible to the substrate-attached surface of the cells. Yellow color in the overlays in C, F, I marks colocalized protein. (L) The lack of yellow indicates the absence of colocalization of laminin subunits. Bar, 10 μm .

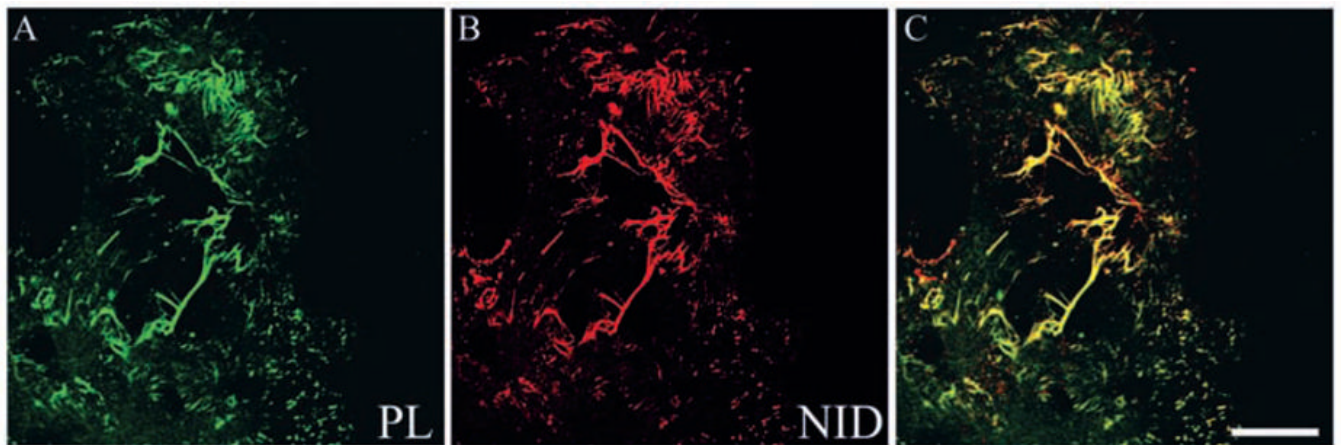


Fig. 3.

Perlecan and nidogen colocalize in the matrix of AECs maintained in vitro. AECs at 4 days after isolation were processed for double-label indirect immunofluorescence using a monoclonal antibody against perlecan (A) and an antiserum against nidogen (B). Confocal laser-scanning images of the cells were generated at a focal plane as close as possible to the substrate-attached surface of the cells. The yellow color in the overlay in C indicates where perlecan and nidogen co-distribute. Bar, 10 μ m.

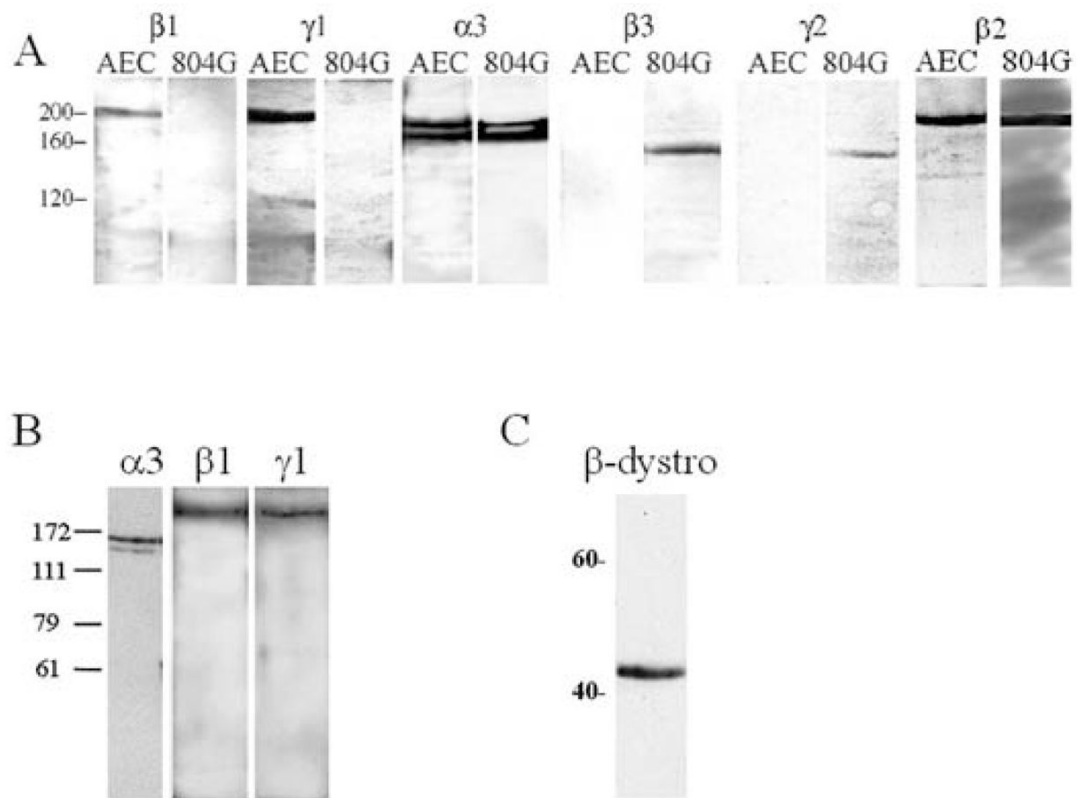


Fig. 4.

Laminin subunit and dystroglycan expression by AECs in vitro. (A) Extracts of AECs (at 4 days after plating) and the rat bladder-cell line 804G were prepared for western immunoblotting using antibodies against $\beta 1$, $\gamma 1$, $\alpha 3$, $\beta 3$, $\gamma 2$ and $\beta 2$ laminin subunits. (B) A matrix preparation derived from AECs at 4 days after plating was processed for immunoblotting using antibodies against the $\alpha 3$, $\beta 1$ and $\gamma 1$ laminin subunits. (C) An immunoblot of an AEC extract at 4 days after plating was processed using the β -dystroglycan antibody 8D5. Molecular weight standards are marked at the left of each series of blots.

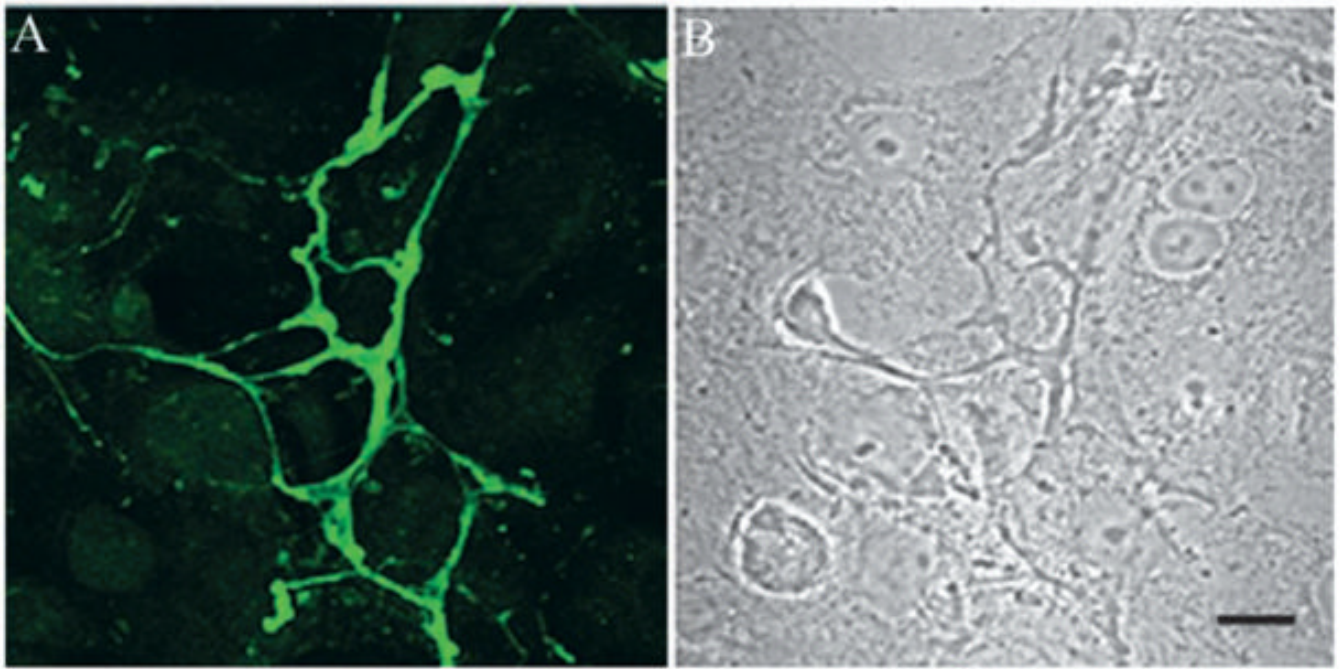


Fig. 5. Laminin matrix organization of AECs maintained on a deformable substrate in vitro. AECs, maintained for 4 days on elastomer membranes, were prepared for confocal indirect immunofluorescence microscopy using antibodies against the $\alpha 3$ laminin subunit (A). Notice the fibrillar arrays of matrix proteins recognized by the antibodies. (B) Phase-contrast image of the cells shown in A. Bar, 10 μm .

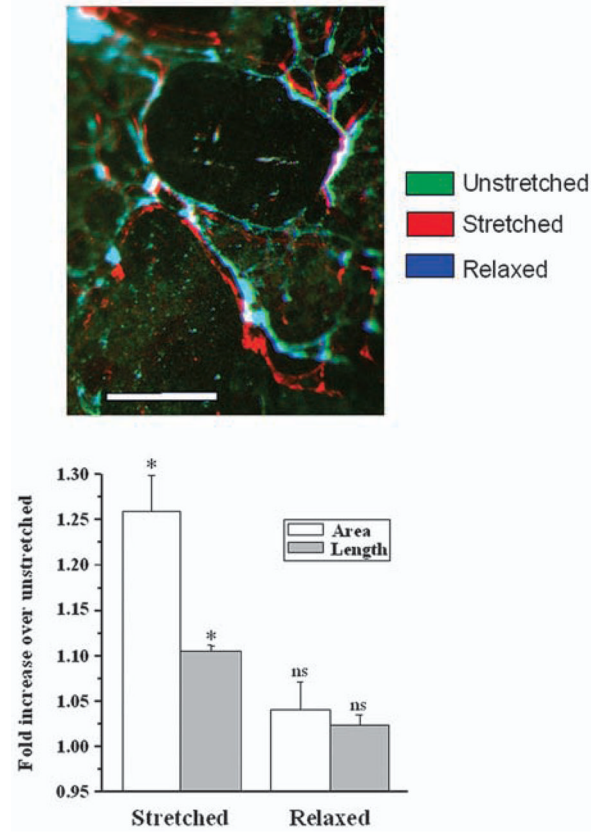
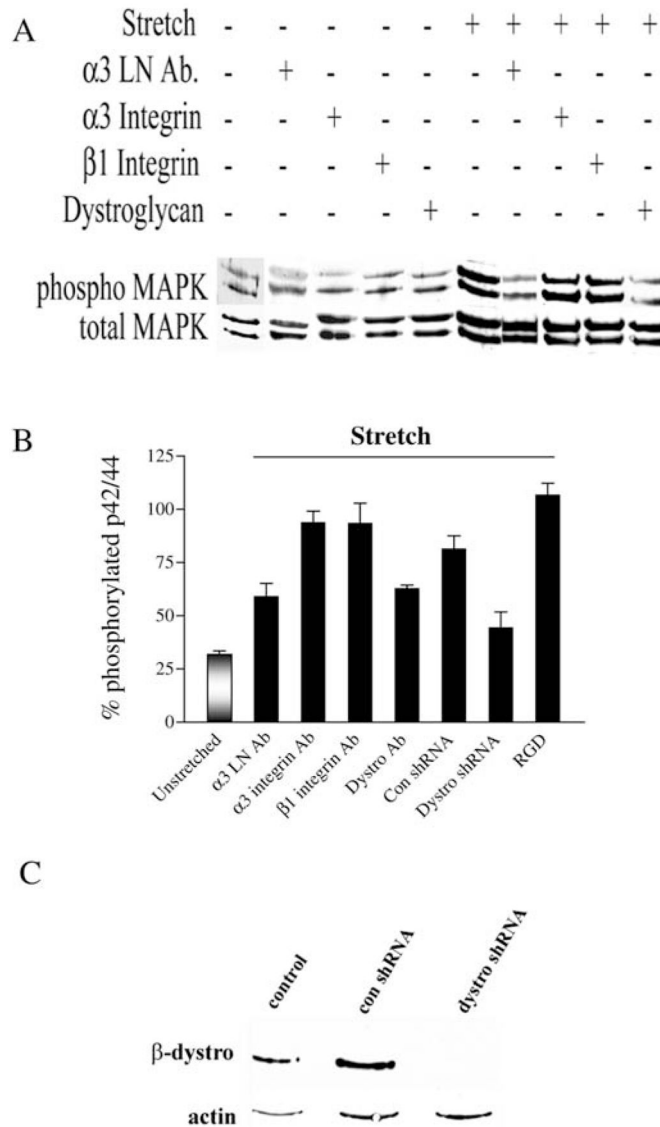


Fig. 6.

Laminin fibers in the matrix of AECs undergo deformation upon stretching. (A) The $\alpha 3$ laminin subunit in native matrix of AECs maintained on an elastomer membrane was immunostained and then the membrane was mounted on the stage of a fluorescent microscope. The membrane was then subjected to cyclic stretching for 10 minutes and then allowed to relax. Images of matrix were captured before, during and after stretching, and colorized in green, red and blue, respectively, as indicated in A. An overlay of the color images is shown. (B) Graphical representation of the changes in area enclosed by the matrix fiber network and fiber length during stretching and following stretching (relaxed). Each measurement is relative to that of unstretched matrix and represents eight different lengths and areas in three independent trials. *, $P < 0.001$. Bar, 10 μm (A).

**Fig. 7.**

The role of matrix molecules and their associated proteins in stretching-mediated signaling. AECs maintained for 4 days on elastomer membranes were subjected to 10% stretching at 30 cycles per minute for 10 minutes. (A) Immunoblots of extracts of AECs, either unstretched (-) or subjected to the stretch regimen (+), probed first with antibodies against phosphorylated MAPK. The same blots were then reprobed with antibodies against total MAPK. The blots are representative of at least three separate trials. The static and stretched cells were incubated in the presence (+) or absence (-) of antibodies that functionally inhibit the $\alpha 3$ laminin subunit ($50 \mu\text{g ml}^{-1}$), $\alpha 3$ integrin ($50 \mu\text{g ml}^{-1}$), $\beta 1$ integrin ($50 \mu\text{g ml}^{-1}$) or dystroglycan ($40 \mu\text{g ml}^{-1}$), as indicated, for 18 hours before stretching. The bar graphs in B are quantifications of the densitometric scans of immunoblots of extracts derived from AECs in three separate trials following 10% stretching at 30 cycles per minute for 10 minutes in the presence of various cell-surface and matrix antibody antagonists or reagents, or following infection with adenovirus encoding either control or dystroglycan shRNA. Blots were probed first with antibodies against activated p42/p44 MAPK and then with antibodies against total p42/p44 MAPK. In each case, the extent of phosphorylation of p42/p44 MAPK in stretched AECs was

normalized to the total level of MAPK in the same sample. The percentage phosphorylation was calculated relative to untreated, stretched values in each set of studies. Error bars indicate standard deviations. (C) AECs were infected with adenovirus encoding either control or dystroglycan shRNA at 2 days after plating. 24 hours later, the cells were washed and incubated for 18 hours in serum-free medium. Extracts of uninfected and infected cells were then prepared for SDS-PAGE and immunoblotting using a monoclonal antibody against β -dystroglycan. The same immunoblot was then reprobbed with an antibody against actin.

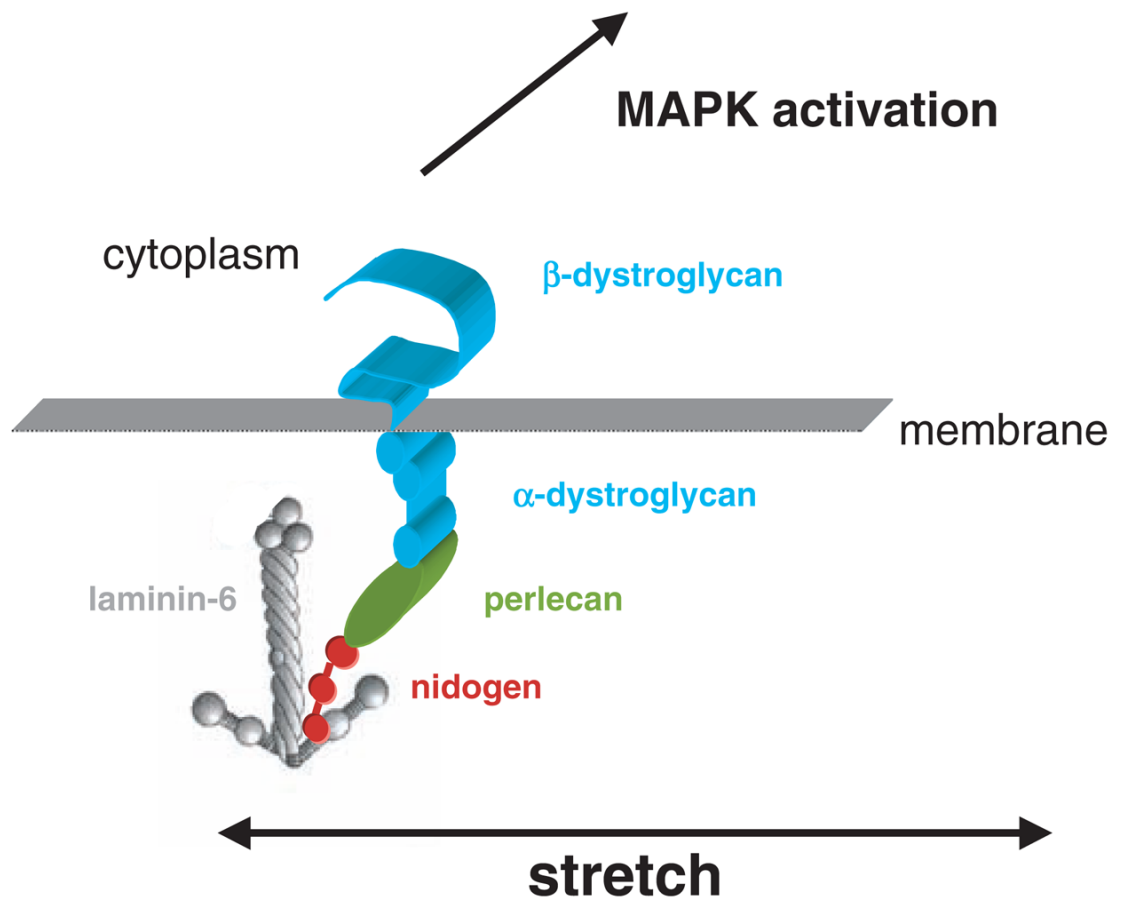


Fig. 8. The organization of matrix components and matrix receptors that mediates outside-in mechanical signaling in AECs. Stretching deflects matrix fibers that (as our data indicate) transduce signals via dystroglycan at the surface of AECs.